ANGULAR CORRELATION OF GAMMA RAYS FOR POSITRONS ANNIHILATING IN SOME OXYGEN-LIQUID MIXTURES AND IN FERROMAGNETIC SUBSTANCES

A Thesis

Submitted to the

Faculty of Graduate Studies

University of Manitoba

in partial fulfillment of the

requirements of the degree of

Master of Science

by

Shu-yuan Chuang

Winnipeg, Canada

August 1965

TABLE OF CONTENTS

LIST OF FIGURES

LIST OF TABLES

ACKNOWLEDGMENTS

The author wishes to take this opportunity to express his sincere thanks to Dr. B. G. Hogg for suggesting the problem and for his patient guidance and constant encouragement throughout the whole development of this work.

Thanks are due to Dr. D. P. Kerr and Mr. A. M. Cooper for many helpful discussions and for their assistance during the early part of these experiments.

Acknowledgment is due also to Dr. A. H. Morrish for suggesting the use of perovskite crystals in the last part of these experiments, and to Dr. R. B. Ferguson and Mr. R. I. Gait for their assistance and discussions in the determination of the structure of the crystals.

Finally the author wishes to acknowledge the kindness of his wife for typing this thesis.

This work was supported by the National Research Council of Canada and the American Chemical Society.

ABSTRACT

The angular correlation of gamma rays for positrons annihilating in a number of oxygen-liquid mixtures and in two magnetized substances have been performed. The angular correlation data of O_2-liquid mixtures were converted to momentum distributions of the annihilating electron-positron pairs. It was found that the momentum distribution shapes were nearly independent of the amount of dissolved oxygen, while the long life time τ_2 is severely quenched by dissolved oxygen. The quenching mechanism of ^3S--^1S conversion was rejected and the formation of positronium compounds postulated to account for the experimental angular correlation data.

Preliminary investigations on polarized positron annihilation in magnetized Alnico and $(La_{.70}Pb_{.30})MnO_3$ have been reported. It was confirmed that the shape of the polarization curve for Alnico was in agreement with the shape of polarization in Fe which indicated an antiparallel conduction band polarization.

CHAPTER 1

INTRODUCTION

When a positron enters a condensed medium it may annihilate directly with an electron or it may capture an electron to form positronium in the triplet or the singlet state. Triplet or singlet positronium is formed depending on whether the spins of the positron and the electron are parallel or antiparallel. The singlet state annihilates with the emission of two quanta, while the triplet state annihilation is accompanied by a three-quantum emission. Direct annihilations and annihilations from the singlet state of positronium have a mean life time $\sim 1.25 \times 10^{-10}$ seconds. This is known as the τ_1-component. The mean life time of the triplet positronium with a three-quantum annihilation is $\sim 1.4 \times 10^{-7}$ seconds.

Associated with two-quantum annihilation, there is also observed in a condensed medium a second longer life time of the order of 10^{-9} seconds. It is known as the τ_2-component. The τ_2-life time is interpreted as arising from "pick off" annihilation from the ^3S state (Dresden 1954; Wallace 1955). The so-called "pick off" process may occur in which the positron annihilates by two-quantum

emission with an atomic electron whose spin state relative to it is singlet.

When a positron-electron pair at rest annihilates with the formation of two-photon emission, an energy of $2mc^2$ is released where m is the mass of electron and c is the velocity of light. To conserve momentum, these two photons (each will have a momentum mc) are emitted at 180° to each other in the center of mass system. If the annihilating pair has some momentum at the time of annihilation, then the photon pair will be emitted at an angle differing from 180° by an amount of the order of v/c where v is the velocity of the center of mass of the annihilating pair. For the low velocities the departure of the angle between the direction of the photons from 180° is proportional to the component of momemtum of the annihilating pair which is parallel to the bisector of the propagation directions. Thus, one may measure the angular distribution of annihilation photons and convert this to a momentum distribution of the annihilating positron-electron pairs (Stewart 1957).

The study of angular correlation of two-photon annihilation of positrons in matter has been investigated

by many investigators and has become a useful tool in study of atomic and molecular properties. The original measurements of the angular correlation of photons from positron annihilation were made by Beringer and Montgomery in 1942. The first detailed theoretical and experimental investigations employing far greater precision have been done by de Benedetti et al. in 1950. Following this, both Warren et al. (Argyle and Warren 1951; Warren and Griffiths 1951; and Erdman 1955) and Maier-Leibnitz (1951) also measured the angular correlation of photons from annihilations in various elements and compounds.

Most of the extensive measurements with metals and alkali halides have been done by Stewart et al. (Stewart and Green 1955; Green and Stewart 1955; Stewart 1955;1957; Stewart and Pope 1960; Donaghy and Stewart 1964) and by de Benedetti and co-workers (Lang, de Benedetti, and Smoluchowski 1955; Lang, de Benedetti 1957). It was found that the half-width of the angular distribution was a good measure of the Fermi energy of light metals, and that the angular distributions can be converted to the momentum distributions of the annihilating positron-electron pairs. Page and co-workers (Page, Heinberg, Wallace,

and Trout 1955; Page and Heinberg 1956) also measured positron annihilations in organic and amorphous substances. They have shown that angular correlation measurements give information about the mechanism of positron annihilation in solids and about the electrons of the solid with which the positrons annihilate.

In the study of the factors affecting the formation and destruction of positronium in matter, de Zafra (1958) has reported some measurements of the angular correlation of photons from positron annihilation in condensed materials under varying conditions of temperature, pressure and phase, and in the presence of certain types of impurities. It was found that the underlying cause of the density-temperature effect seemed to be simply a variation in fraction of positrons forming positronium. The influence of paramagnetic ions in causing $^3S \longrightarrow {}^1S$ conversion in positronium by electron exchange was also investigated.

In 1960, Trumpy has also measured the angular correlation of photons from positron annihilation in aqueous solutions. It was confirmed that the amount of singlet positronium formed is influenced by two processes: a reduction of positronium due to electron capture by oxidizing substances

and an increase of the $^3S \longrightarrow {}^1S$ conversion due to electron exchange with paramagnetic ions. The oxidation potential of positronium was found to be very nearly zero, and the conversion rate was proportional to the number of unpaired electrons on the dissolved ions.

Kerr (1964) has measured the angular correlation of photons from positron annihilation in a number of organic liquids with increased experimental accuracy. The angular correlation data have been converted successfully to momentum distributions of the annihilating pairs in contrast to previous experiments in liquids where the experimental accuracy had not been sufficient to allow such a conversion. It was found that there are two momentum components which appear in the momentum distributions whenever positronium is formed. It was confirmed that the intensity of the low momentum component is equal to one third of the intensity of the long lived component. He also observed that the high momentum component was a direct measure of the momentum distribution of the electrons involved in the annihilation process.

Recently some measurements of the time spectra have been reported (Lee and Celitans 1965; Kerr, Cooper, and

Hogg 1965) that the long lifetime (τ_2) for positron annihilation in some organic liquids is severely quenched when oxygen is dissolved in the liquid. This has been interpreted previously as being due to $^3S \longrightarrow {}^1S$ conversion by paramagnetic oxygen. Hogg et al. (Kerr, Cooper, and Hogg 1965) has shown that the conversion mechanism was not responsible for the quenching of τ_2 in hexane.

In this work it will be shown again that the quenching of τ_2 in a number of O_2-liquid mixtures is not due to the $^3S \longrightarrow {}^1S$ conversion. It will be interpreted as being probably due to the formation of positronium compounds.

In the last part of this work, some preliminary investigations on polarized positron annihilation in ferromagnets will be reported. The positron annihilation angular correlation method was first used by Hanna and Preston (1958) to investigate the momentum distribution of electrons responsible for ferromagnetism. In order to obtain information concerning the state of polarization of these electrons, recently some investigators (Mijnarends and Hanbro 1964; Berko and Zuckerman 1964) have repeated these measurements in iron and nickel. It was found that the conduction electrons in ferromagnets were polarized

antiparallel to 3d electrons, and that the interpretation of the polarization experiments was somewhat model dependent. A series of experiments on a perovskite ferromagnetic substance ($La_xPb_{1-x}MnO_3$) without conduction electrons have been performed. The same ferromagnetic substance with various conductivities (by changing temperature) is presently under investigation in our laboratory.

FIG 1

FLOW DIAGRAM FOR POSITRON ANNIHILATION

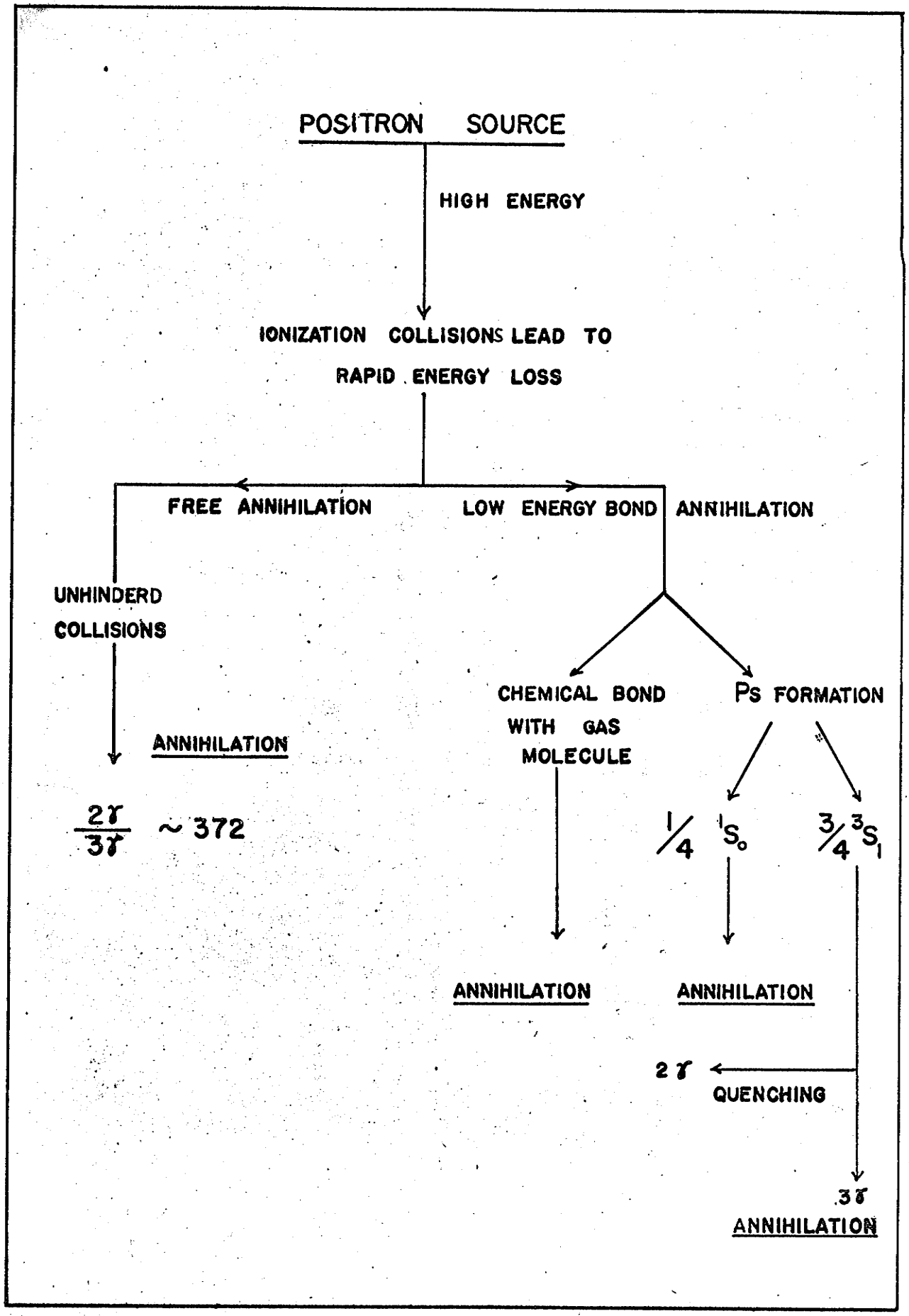
POSITRON SOURCE
HIGH ENERGY
IONIZATION COLLISIONS LEAD TO
RAPID ENERGY LOSS
FREE ANNIHILATION
LOW ENERGY BOND ANNIHILATION
UNHINDERD
COLLISIONS
ANNIHILATION
2γ / 3γ ~ 372
CHEMICAL BOND
WITH GAS
MOLECULE
Ps FORMATION
1/4 1S0
3/4 3S1
ANNIHILATION
ANNIHILATION
2γ
QUENCHING
3γ
ANNIHILATION

CHAPTER 2

APPARATUS

The angular correlation apparatus consisted of two main parts---the mechanical and electronics components. A detail of arrangements of the apparatus will be described as follows.

Mechanical:

A diagram of the mechanical parts of the angular correlation apparatus is shown in Figure 2. The basic mechanical features are the source and sample housing, with surrounding collimating slits and two gamma ray detectors with their collimating slits. All these components were mounted on two parallel 3" by 6" aluminium I-beams approximately 20 feet long. The two gamma tay detectors were mounted on two ends of the I-beams. One detector was fixed and the other was movable. The source and the sample were shielded in a lead castle, being placed on the middle of the I-beams, with collimating slits facing each detector.

The widths of the collimating slits of the lead castle were 0.1" and 0.4", facing the fixed detector

and the movable detector respectively. The reason for a wider slit, on the side of the movable detector, is that the movable detector had to be permitted to see the sample directly from a variety of positions, The purpose of these collimating slits was to reduce the amount of scattered radiation reaching the detectors as well as to shield the detectors from the source.

The fixed gamma ray detector ("B" in Fig. 2) and its collimating slits were mounted on a brass plate 265cm from the source. This detector was rather heavily shielded by 3" thick lead blocks to cut down the accidental background rate from scattered gamma rays and from other sources in the laboratory.

The movable detector ("A" in Fig. 2) and its collimating slits were mounted on a steel plate, placed 265cm on the other side of the sample, driven by a worm screw between a set of linear rails. Here a "Slo-Syn" 600 ounce-inch reversible motor was used.

The collimating slits of these detectors were made from 2½" thick lead blocks. This thickness was sufficient to stop most of all gamma rays from this

experiment. The width of slits could be changed by inserting metal shims of the appropriate thickness between the lead blocks.

To keep the collimating slits of the detectors aligned towards the sample as the movable detector moved to different positions, an aluminium beam, which was reinforced by a set of three steel cables to both ends of the beam, was extended from the front of the rotatable steel plate to a pivot point directly under the sample housing on a vertical axis through the sample. To allow for the slight increase in the distance from the detector to the pivot point as the detector was moved off the center position, the end of the aluminium beam was permitted to slide freely in a hole in the pivot shaft.

To define the position of the sample and align the apparatus a fine wire was stretched between the slits of the two detectors which were in the position of 180 degree line. The position of the sample was adjusted so that its face was just in contact with the wire. Checks were made periodically on the alignment, to guard against any accidental shifting of the equipment. (If the slits were shifted slightly out of line, a change in the peak

position of the angular correlation curves would be observed. But such a change would not affect the final experimental results.)

A check was also made on the constancy of the pitch of the worm screw by measuring the distance that the whole slit system of the movable detector moved with each rotation of the screw, The slit system moved 2.54mm with each rotation. A maximum variation of 0.03mm of one rotation was obtained, but a deviation of this magnitude would not affect the experimental results noticeably.

Electronics:

A block diagram of electronics is shown in Fig. 3. The detectors were Integral Assembly model 16MB4/A-X and consisted of 4" diameter, 1" thick NaI (Tl) crystals mounted on 5018 HB photomultipliers with mu-metal shields. A positive high voltage (1000 volts) was provided for photomultipliers by a Hamner N401 high voltage supply. Negative pulses which have the order of one volt in amplitude, from the cathode followers in the detector heads were fed to simple amplifiers (Kerr 1964) through 1059 Amphenol coaxial cable, and were amplified about eighteen times and shortened to approximately 1 microsecond.

The power for the amplifiers and cathode followers in the detector heads was provided by a highly regulated 250-volt D.C. power supply based on a National Bureau of Standards design.

Pulses from the amplifiers were fed to single channel pulse height analysers set to select gamma rays in the energy range between 0.1 and 0.5 Mev. The fast rising narrow pulses (0.2 micro-seconds) were sent to a coincidence unit which had a resolving time of less than 0.5 microseconds. The pulse height analysers and the coincidence unit have been described previously (Naqvi 1961). A Technical Measurement Coorporation Model SG-3A scaler was used to record the number of coincidences.

When 1000 counts have been accumulated on the scaler, through the "automatic unit" (de Zafra 1958; Kerr 1964), the track motor is started and moves the movable detector to its next position, simultaneously, the scaler stops counting as the motor is running, and the scaler starts counting again as soon as the motor stops while the detector has been driven to its new position. When the detector moves to the predetermined end of its run in either direction (eg.12 mr in each

side), it will reverse the direction automatically by reversing switches in the automatic unit system. A Simplex Time Printer Model ET-100 was used to print out the time interval during each 1000 counts of coincidences.

All the electronic instruments were powered by a model 2000 S Sorensen A.C. Voltage regulator.

Preparation of Positron Source:

A 12 millicuries Na^{22} source in the form of NaCl solution obtained from the Radiochemical center, Amersham, England. The source had a high specific activity, 3mc/mg, and was dissolved originally in 6ml. of water.

The source preparation was accomplished as follows: a ½" diameter plastic button on which the Na^{22} was to be deposited was prepared by machining shallow, concentric circular grooves on it. The source was evaporated from solution, drop by drop, on the plastic button mounted on the end of a ½" diameter, 10" long plastic rod, and then covered with a thin piece of mica ($2mg/cm^2$) sealed around the sides of the button with epoxy resin glue. It was estimated that about 10mc of the source was deposited on the plastic button as the evaporation process was finished.

The remainder was left in the original source container, in syringe and in hypodermic needle. Unfortunately, this source was broken by an accident, unexpectedly, during the time of moving it from the radiochemical laboratory in which the source was prepared to our laboratory. The surface of the source was covered again by another piece of mica. The total thickness of the two pieces of mica which had covered the source was about 4mg/cm^2. This thickness of the source covering was still thin enough to obtain a reasonable yield of positrons. But the yield of positrons obtained, was much lower than what we had expected. Soon, it was found that this was due to the self absorption in the source since the salt crystals of Na^{22} were accumulated in one area of the surface of the plastic button during the accident. The source was then opened and redissolved in a small amount of water and deposited on a new plastic button which had been prepared in the same manner as the previous one except the grooves on it were a little more shallow. After the process of transfer was completed, it was estimated that about 20% of activity was lost and appoximately 8mc of Na^{22} was deposited on the new plastic button.

The new plastic button, covering with 2.5 gm/cm^2 thin mica, was mounted on a plastic rod, and then inserted into a brass tube in the side of the source castle and was held in place by a locking screw. To achieve the maximum counting rate, the source was placed as near the sample as possible without the source becoming directly visible to both detectors through the crude collimating slits of the source castle.

FIGURE 2

MECHANICAL PART OF THE ANGULAR CORRELATION APPARATUS

A. Movable detector
B. Fixed "
C. Positron source
D. Sample tank
E. Reversing switches
F. Cam operated switch
G. Motor

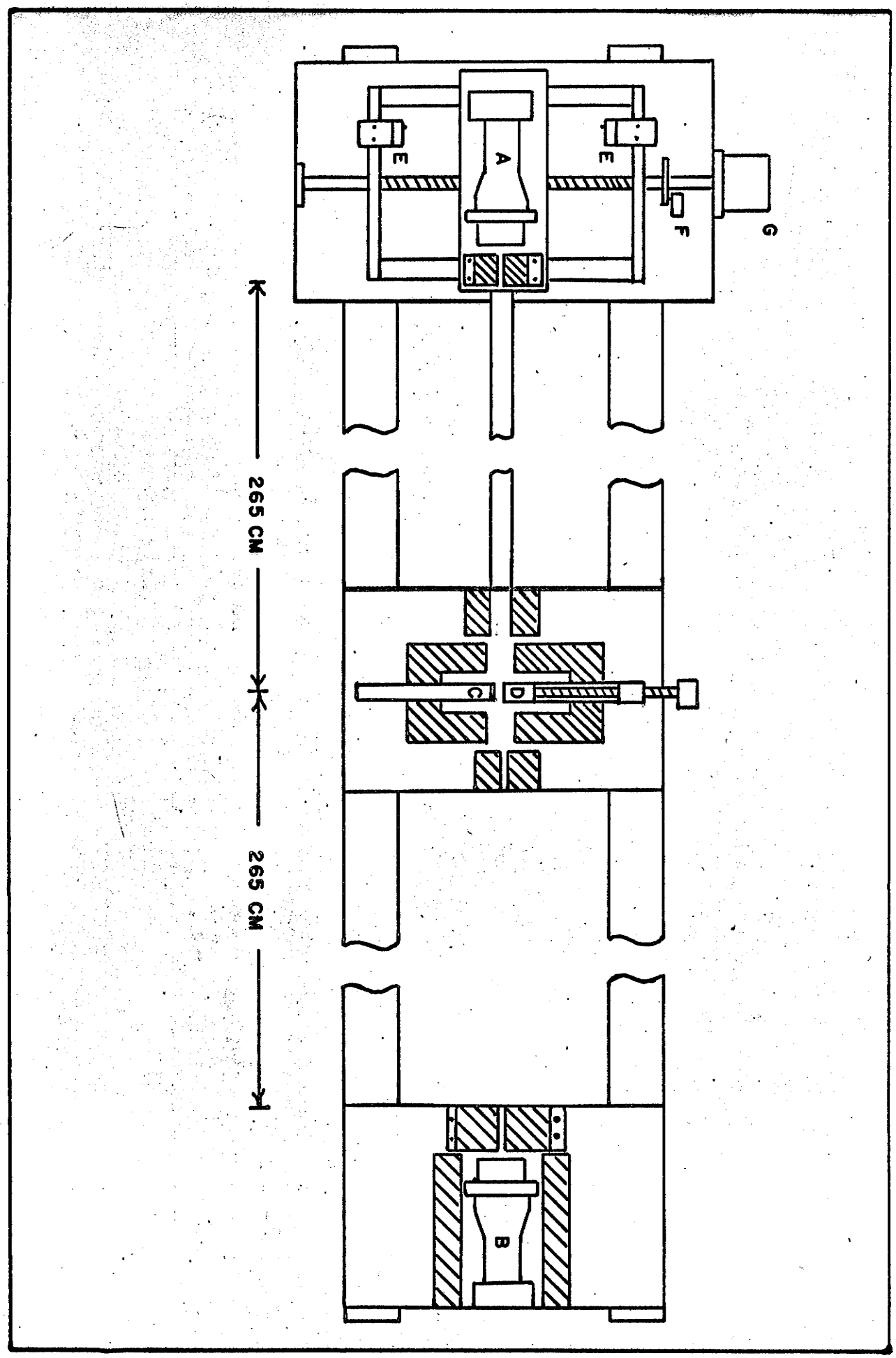
A
B
C
D
E
E
F
G
265 CM
265 CM

FIGURE 3

BLOCK DIAGRAM OF THE ANGULAR CORRELATION APPARATUS

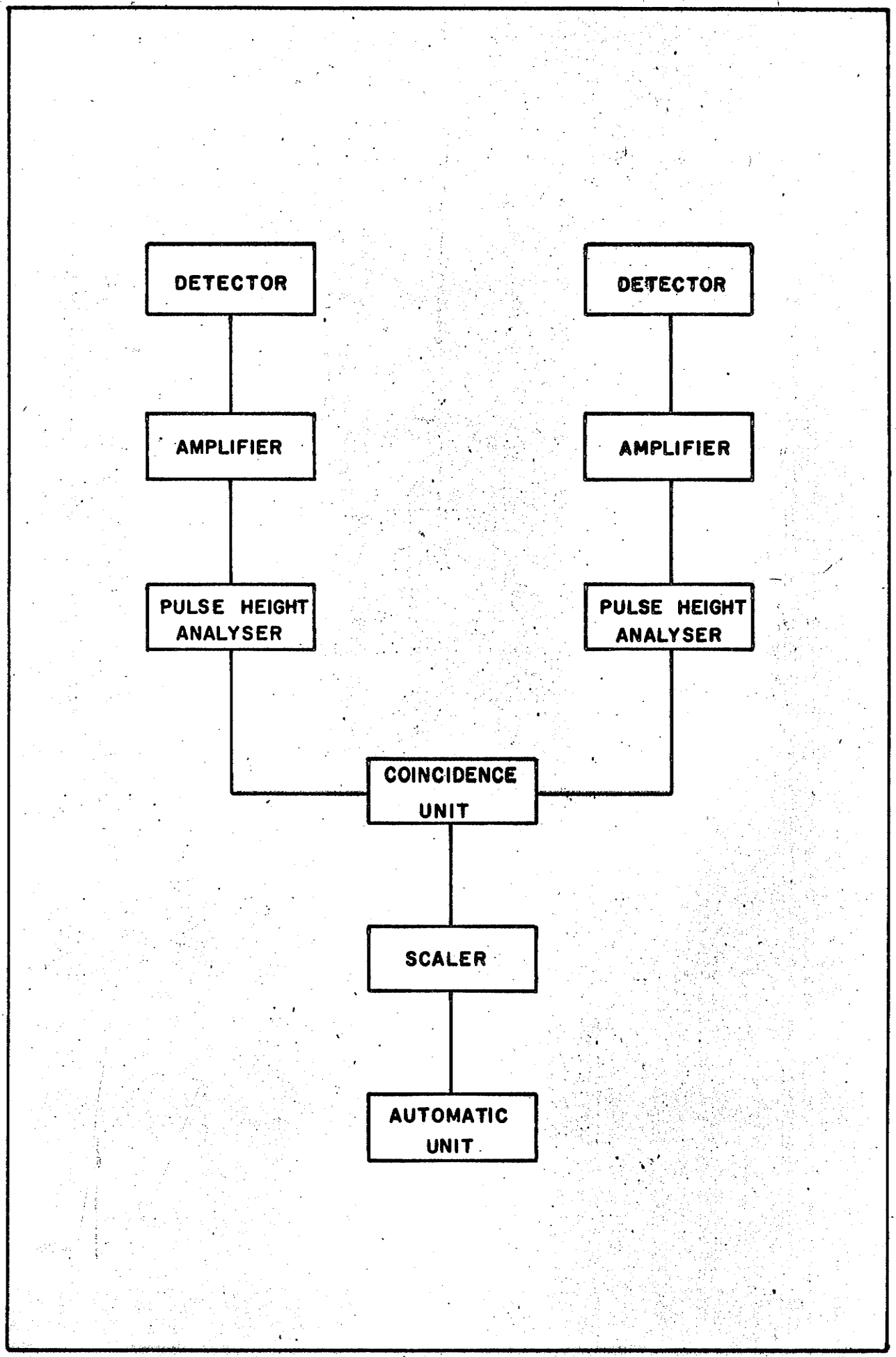
DETECTOR
DETECTOR
AMPLIFIER
AMPLIFIER
PULSE HEIGHT ANALYSER
PULSE HEIGHT ANALYSER
COINCIDENCE UNIT
SCALER
AUTOMATIC UNIT

CHAPTER 3

POSITRON DECAY IN O_2-LIQUID MIXTURES

Data Accumulation and Analysis

Two-photon angular correlation measurements were performed for oxygen-saturated, air-saturated, and degassed samples of the following liquids: hexane and two of its halogen derivatives (ie. fluorohexane and chlorohexane), distilled water, and $NaNO_3$ solution in water (1mole/liter). The oxygen-saturated process was accomplished simply by bubbling oxygen through the sample under investigation. The oxygen concentration for this case was estimated to be about 200cc/liter, while for the air-saturated case it was 40cc/liter (Kerr, Cooper, and Hogg 1965). The degassed process was accomplished by the standard vacuum freeze-thaw technique. The degassed sample was analyzed mass spectrometrically and was found to contain less than 1% of the amount of oxygen present in the air-saturated sample.

All these samples were contained in a small brass tank with a 3/4" vertical face covered with a thin mica sheet (1.5mg/cm^2) so that more than 95% of the incident

positrons could penetrate through the mica-window and annihilate in the liquid sample. The slits in front of the two detectors subtended an angle of 0.60 milliradians. An angular range about 12 milliradians on either side of the 180° line was set for taking the angular correlation curves. At each angle, approximately 20,000 counts were accumulated.

To determine the background counts in the angular distributions, a brass ring which was made in the manner of having the same diameter and the wall thickness of the sample tank and covered with a same thickness of mice sheet was used to perform several runs in place of the sample. The resulting back-ground distribution was fairly broad with a peak at the center. In addition to this background, the chance coincidences which contributed a flat background of approximately 3 counts per minute was also taken into account.

Stewart (1957) has shown that in the experiment with an apparatus having parallel slit geometry, the angular distribution of the annihilation photons can be converted to the momentum distribution as

$$N(p)=a_1\theta\frac{dC(\theta)}{d\theta} \qquad (1)$$

and the corresponding momentum space density is given by

$$\rho(p)=a_2 \frac{1}{\theta} \frac{dC(\theta)}{d\theta} \qquad (2)$$

In these relations a_1 and a_2 are constant factors and $C(\theta)$ is the measured photon coincidence counting rate.

Results of the experiment are given in Figs 4—13, in which all data are presented in three forms:

(a) the angular distribution $C(\theta)$ vs θ,

(b) the momentum space density $\rho(p)$ vs θ,

(c) the momentum distribution $N(p)$ vs θ.

The momentum distribution and the density of the momentum space were calculated from the relations:

$$N(p)=a_1 \left[(\theta_1+\theta_2)/2\right]\left[C(\theta_2)-C(\theta_1)\ /(\theta_2-\theta_1)\right] \qquad (3)$$

$$\rho(p)=a_2 \left[2/(\theta_1+\theta_2)\right]\left[C(\theta_2)-C(\theta_1)\ /(\theta_2-\theta_1)\right] \qquad (4)$$

which is a reasonably good approximation to (1) and (2) since the changes in $C(\theta)$ are small compared to the difference $\theta_2-\theta_1$, between the neighboring points.

The background distribution has been subtracted in angular distribution curves and the curves have been normalized to the same area. The angular resolution of

the apparatus, having a full-width at half maximum of about 0.8 milliradians has not been corrected since this correction is sufficiently small and also in this work we are particularly interested in studying the relative difference between the curves.

Discussion of Results

A. The Narrow Component:

It is evident that two momentum components are generally present in the momentum distributions. The low momentum component is also called the "narrow component" corresponding to the sharp peak found in some of the angular distribution curves $C(\theta)$. The narrow component is interpreted as resulting from the annihilation of singlet positronium, since the positron annihilates with its own bound electron (Ferrell 1956). Direct annihilations and pick-off annihilations contribute to the high momentum component, since these annihilations occur with electrons bound to the molecules in the system.

Since three quarters of the positronium is formed in the triplet state which has three substates ($m=o,\pm1$) and one quarter is formed in the singlet state which has only one ($m=o$) state, the intensity of the low momentum

component, I_L, should be equal to $I_2/3$ where I_2 is the intensity of the long lived component in the time spectra, ie. the amount of triplet positronium formed. Table 1 shows a comparison of I_L and $I_2/3$ in hexane and two of its halogen derivatives, and in every case there is agreement within experimental error. This experimental evidence therefore, substantiates the view that the low momentum component is due to the self annihilation of singlet positronium.

B. Oxygen in Liquids---Evidence for Formation of Positronium Compounds:

The long life time (τ_2) for positron annihilation in some organic liquids is severely quenched when oxygen is dissolved in the liquid (Lee and Celitans, 1965; Kerr, Cooper, and Hogg, 1965). This has been interpreted in general as resulting possibly from a conversion of triplet positronium to the singlet state by paramagnetic oxygen.

As we discussed previously, the narrow component of the momentum distribution is due to the self-annihilation of the singlet-state positronium having an intensity $I_L=I_2/3$. Therefore, if a triplet$\longrightarrow$singlet state conversion is occuring, the narrow component or the low-momentum

component should be enhanced.

The result of this experiment (Figs. 4--13) shows that the shapes of the momentum distributions of hexane, fluorohexane, chlorohexane, distilled water, and $NaNO_3$ solution in water are almost independent, within the experimental error limit, of the amount of dissolved oxygen. This shows that the narrow component I_L is almost constant (and approximately equal to $I_2/3$). This result indicates that little or no $^3S \rightarrow {}^1S$ conversion is taking place. The long life time τ_2 and the intensity I_2 of the same O_2-liquid mixtures were measured with the time spectra apparatus in our laboratery and it was found that the τ_2 is severely quenched and the I_2 is almost constant (in fact, it is slightly increased) as a result of the addition of oxygen (Cooper 1965). Therefore, the conversion mechanism seems not to be responsible for the queching of the τ_2 in O_2-liquid mixtures.

Another possible mechanism resulted in the quenching of the long life time (τ_2) but without producing appreciable change in I_2 is the formation of a positronium compounds (Wallace 1960; Ferrell 1958).

In the study of the quenching effect of oxygen

in liquid argon, Paul (1958) has pointed out that the quenching effect found in liquid argon may be due to the formation of the positronium compound $e^+e^-O_2$. De Zefra (1958), stimulated by work of Berko and Zuchelli (1956), has also found evidence for the positronium compound formation in the study of the quenching effect of Diphenyl-Picryl-Hydrazyl (D.P.H.) in benzene. In their result, which is similar to our result in O_2-liquid experiment, the long life time τ_2 is severely quenched but I_2 remains constant when D.P.H. is dissolved in benzene.

Another point we have to mention here is that the central part of the angular distribution curve in this O_2-liquid experiment, as well as in the case of D.P.H. experiment, was slightly depressed, although it didn't change the narrow component, when oxygen was added. This means that the broad part of the angular distribution is broader, in agreement with the hypothesis of positronium compound formation which indicated that the positronium formed in compound would contribute to the broad part of the angular distribution. Therefore, we would conclude that the O_2 quenching of τ_2 in liquid is most likely due to the formation of positronium compounds rather than the $^3S \longrightarrow {}^1S$ conversion mechanism.

FIGURE 4

ANGULAR DISTRIBUTIONS FOR HEXANE:

(1) Oxygen - saturated Hexane

(2) Air - saturated Hexane

(3) Degassed Hexane

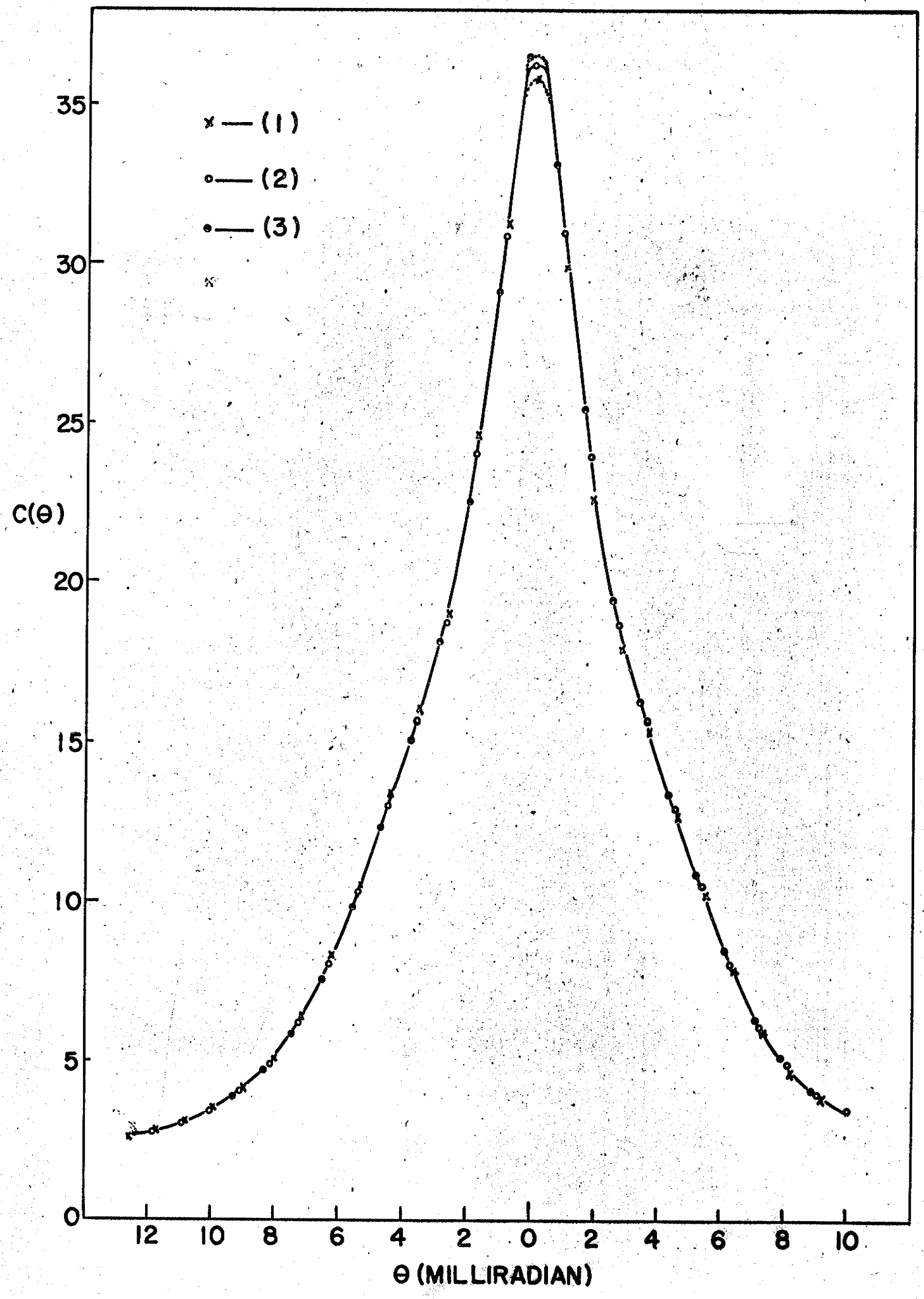
(1)
(2)
(3)
C(θ)
35
30
25
20
15
10
5
0
12
10
8
6
4
2
0
2
4
6
8
10
θ (MILLIRADIAN)

FIGURE 5

MOMENTUM DISTRIBUTIONS $N(p)$ vs θ, AND
MOMENTUM SPACE DENSITY $\rho(p)$ vs θ
FOR HEXANE:

(1) Oxygen - saturated Hexane

(2) Air - saturated Hexane

(3) Degassed Hexane

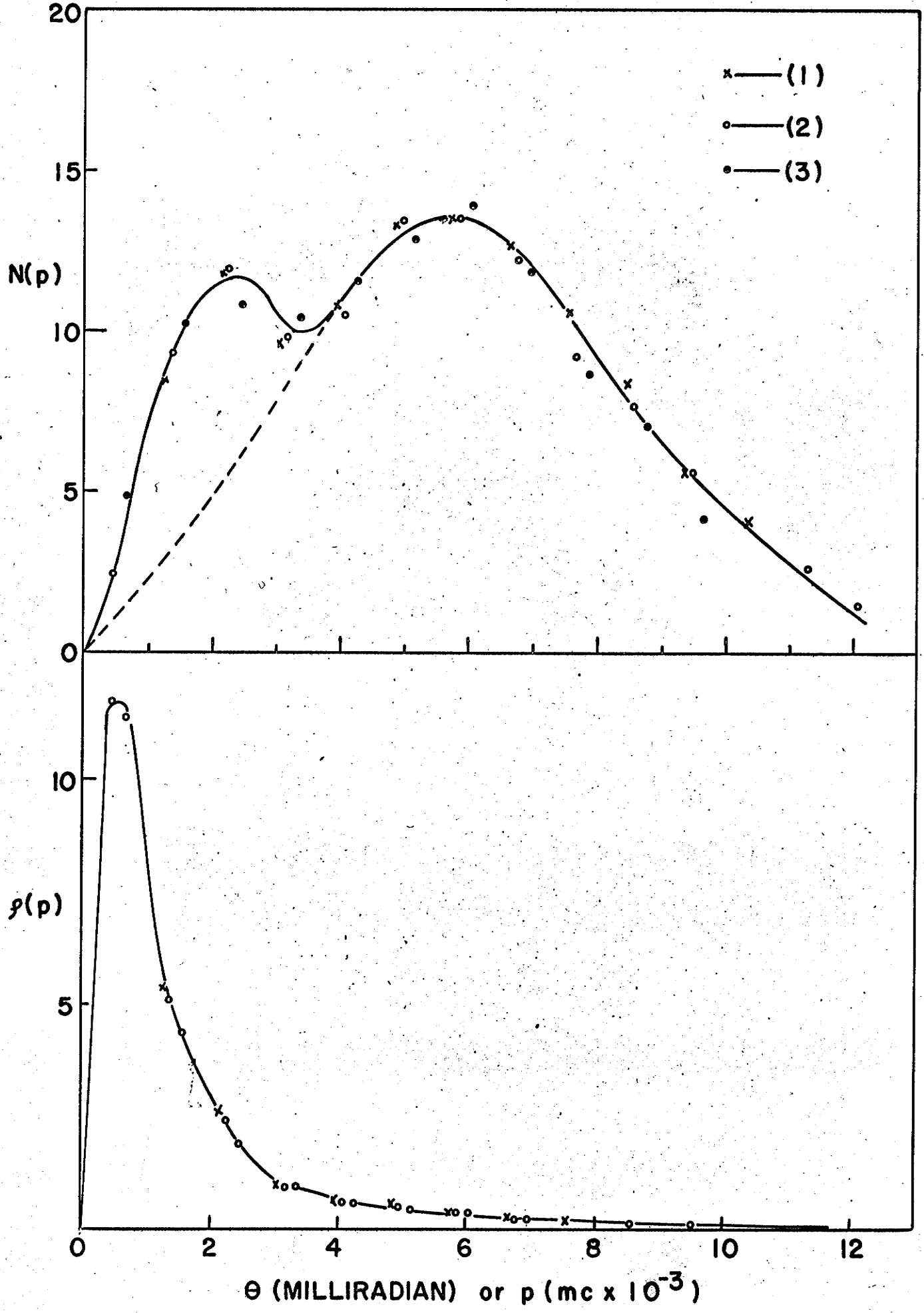
20
15
10
5
0
N(p)
×——(1)
○——(2)
●——(3)
10
5
ρ(p)
0
2
4
6
8
10
12
θ (MILLIRADIAN) or p (mc x 10⁻³)

FIGURE 6

ANGULAR DISTRIBUTIONS FOR FLUOROHEXANE:

(1) Oxygen - saturated Fluorohexane

(2) Air - saturated Fluorohexane

(3) Degassed Fluorohexane

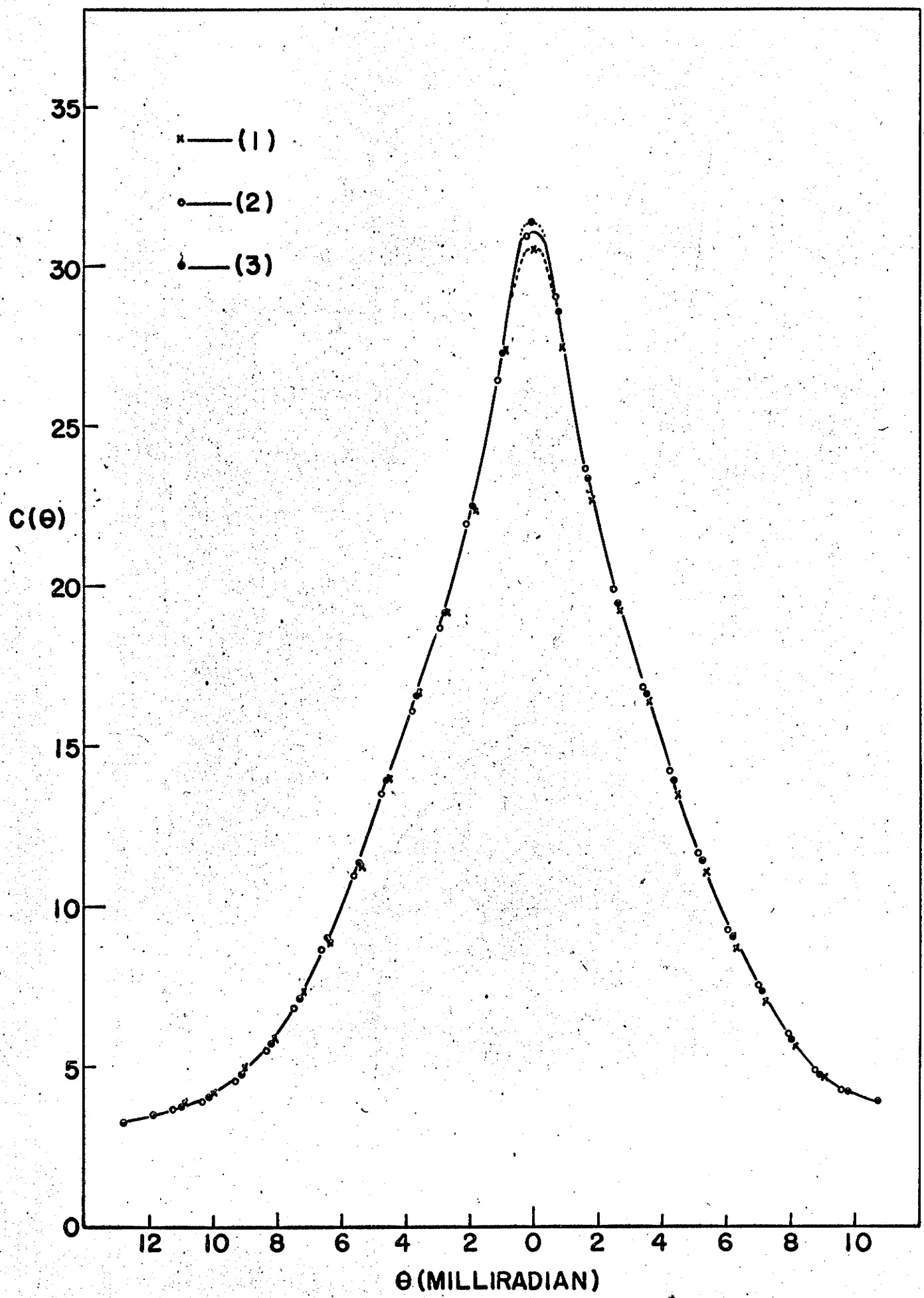
(1)
(2)
(3)
C(θ)
35
30
25
20
15
10
5
0
12
10
8
6
4
2
0
2
4
6
8
10
θ (MILLIRADIAN)

FIGURE 7

MOMENTUM DISTRIBUTIONS N(p) vs θ, AND MOMENTUM SPACE DENSITY $\rho(p)$ vs θ

FOR FLUOROHEXANE:

(1) Oxygen-saturated Fluorohexane

(2) Air-saturated Fluorohexane

(3) Degassed Fluorohexane

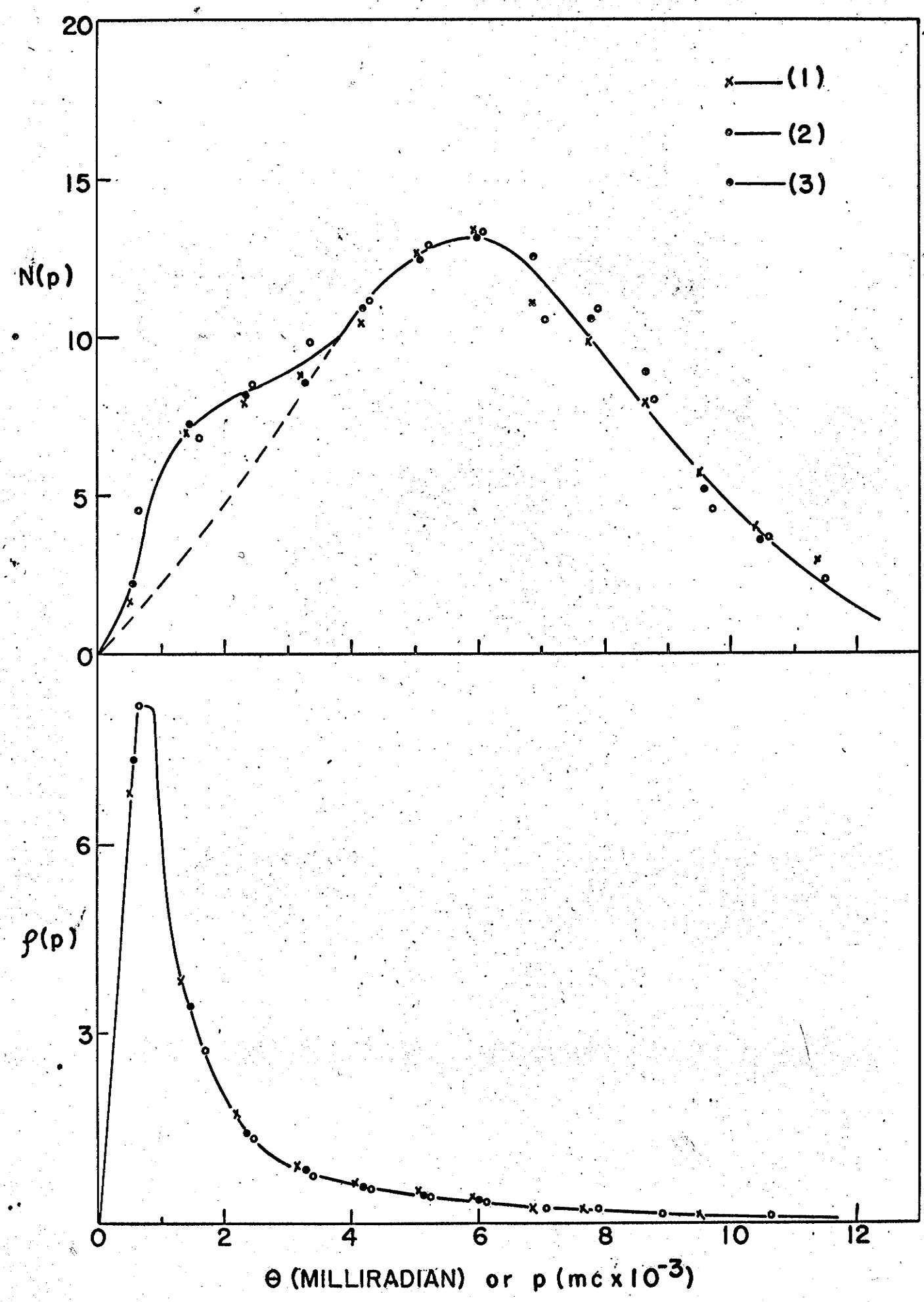
20
15
10
5
0
N(p)
×——(1)
○——(2)
•——(3)
6
3
ρ(p)
0
2
4
6
8
10
12
Θ (MILLIRADIAN) or p (mc x 10^-3)

FIGURE 8

ANGULAR DISTRIBUTIONS FOR CHLOROHEXANE

(1) Oxygen-saturated Chlorohexane

(2) Air-saturated Chlorohexane

(3) Degassed Chlorohexane

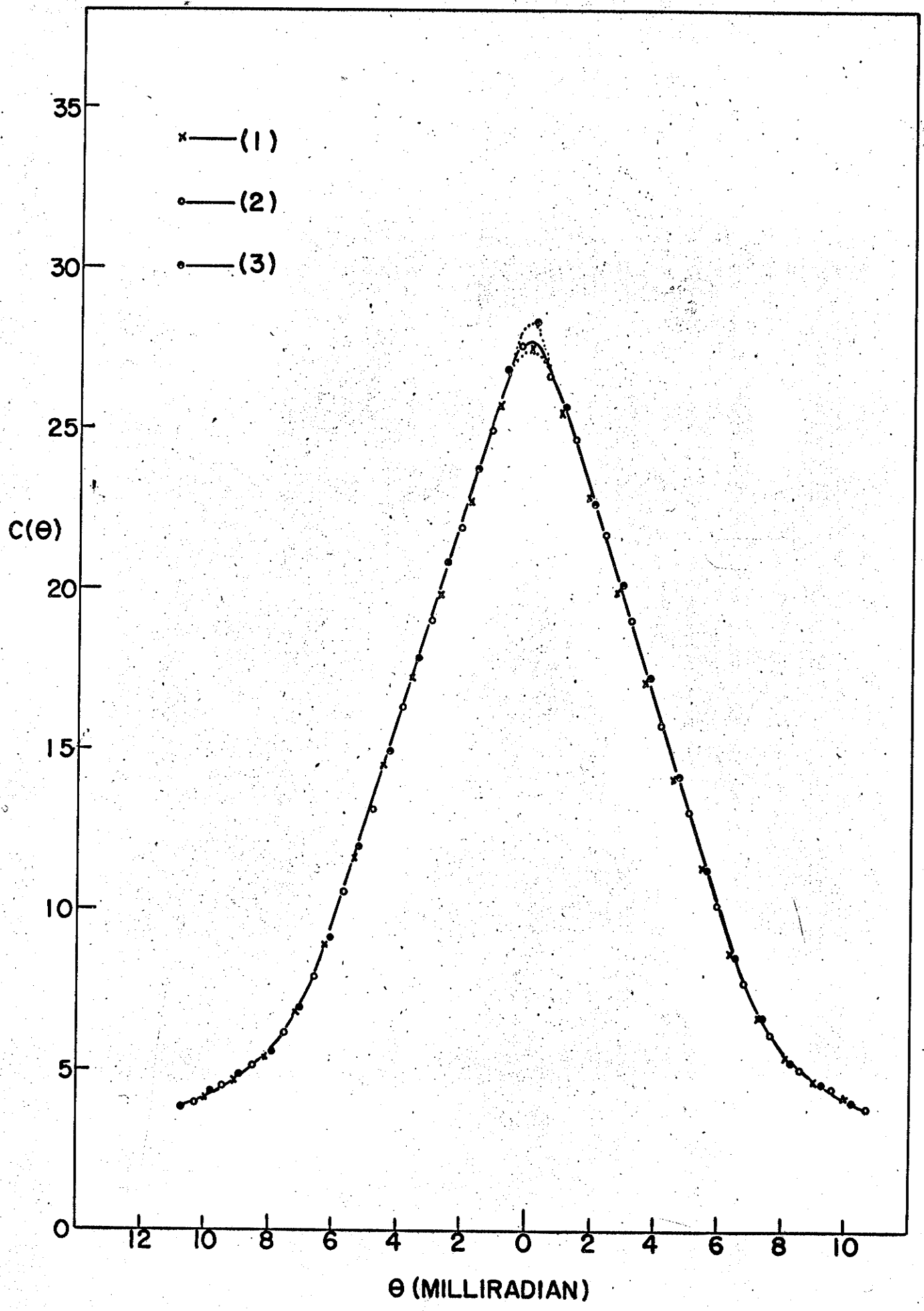
×——(1)
○——(2)
●——(3)
35
30
25
20
15
10
5
0
C(θ)
12
10
8
6
4
2
0
2
4
6
8
10
θ (MILLIRADIAN)

FIGURE 9

MOMENTUM DISTRIBUTIONS N(p) vs θ, and
MOMENTUM SPACE DENSITY $\rho(p)$ vs θ
FOR CHLOROHEXANE:

(1) Oxygen-saturated Chlorohexane
(2) Air-saturated Chlorohexane
(3) Degassed Chlorohexane

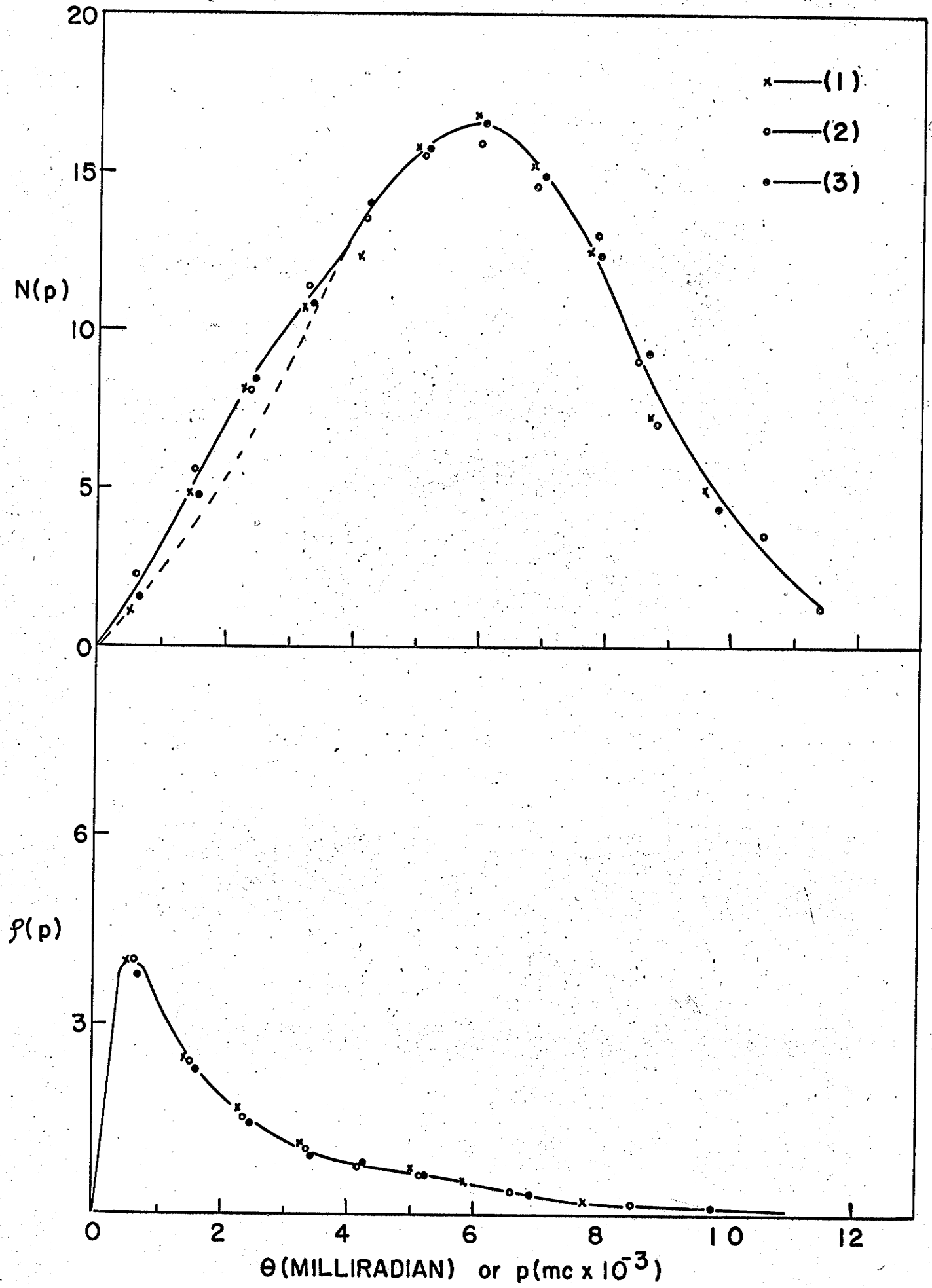
20
15
10
5
0
N(p)
×——(1)
○——(2)
•——(3)
6
3
f(p)
0
2
4
6
8
10
12
θ(MILLIRADIAN) or p(mc x 10⁻³)

FIGURE 10

ANGULAR DISTRIBUTIONS FOR DISTILLED WATER

(1) Oxygen-saturated Water

(2) Air-saturated Water

(3) Degassed Water

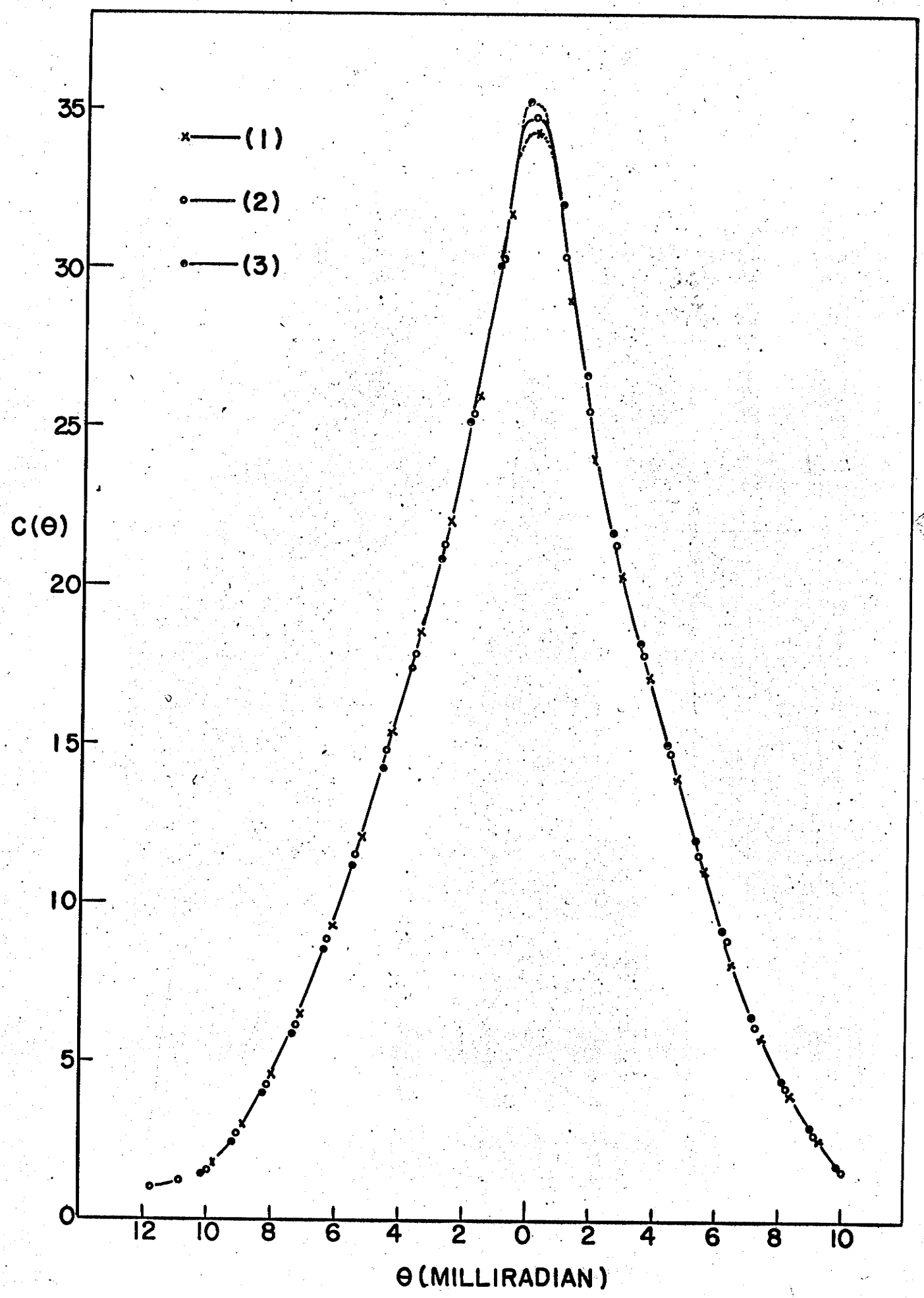
(1)
(2)
(3)
C(θ)
35
30
25
20
15
10
5
0
12
10
8
6
4
2
0
2
4
6
8
10
θ (MILLIRADIAN)

FIGURE 11

MOMENTUM DISTRIBUTIONS $N(p)$ vs θ, and
MOMENTUM SPACE DENSITY $\rho(p)$ vs θ
FOR DISTILLED WATER

(1) Oxygen-saturated Water
(2) Air-saturated Water
(3) Degassed Water

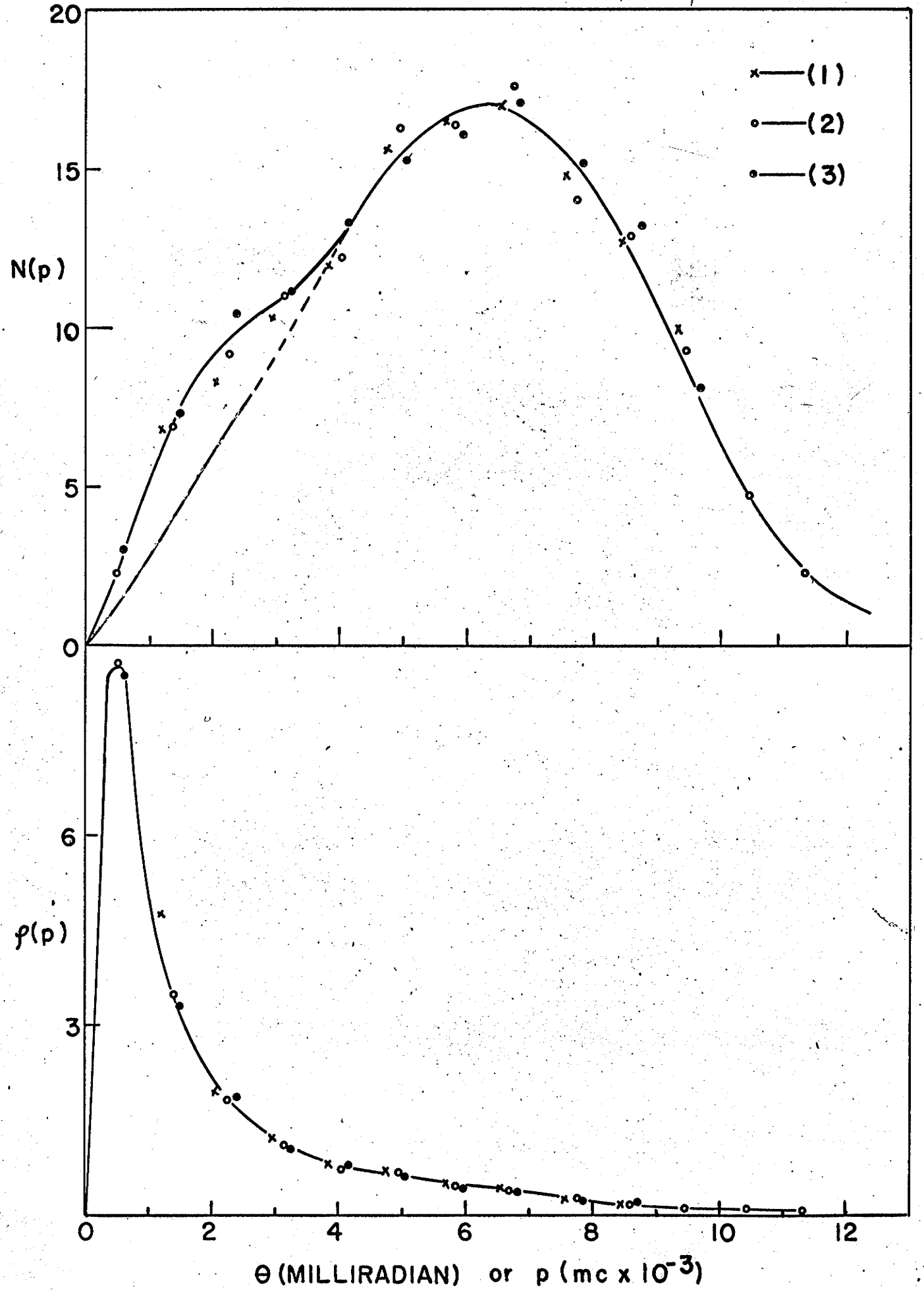
20
15
10
5
0
N(p)
×——(1)
○——(2)
○——(3)
6
3
p(p)
0
2
4
6
8
10
12
θ (MILLIRADIAN) or p (mc x 10⁻³)

FIGURE 12

ANGULAR DISTRIBUTIONS FOR $NaNO_3$ SOLUTION IN WATER (1 MOLE/LITER)

(1) Oxygen-saturated $NaNO_3$ Solution

(2) Air-saturated " "

(3) Degassed " "

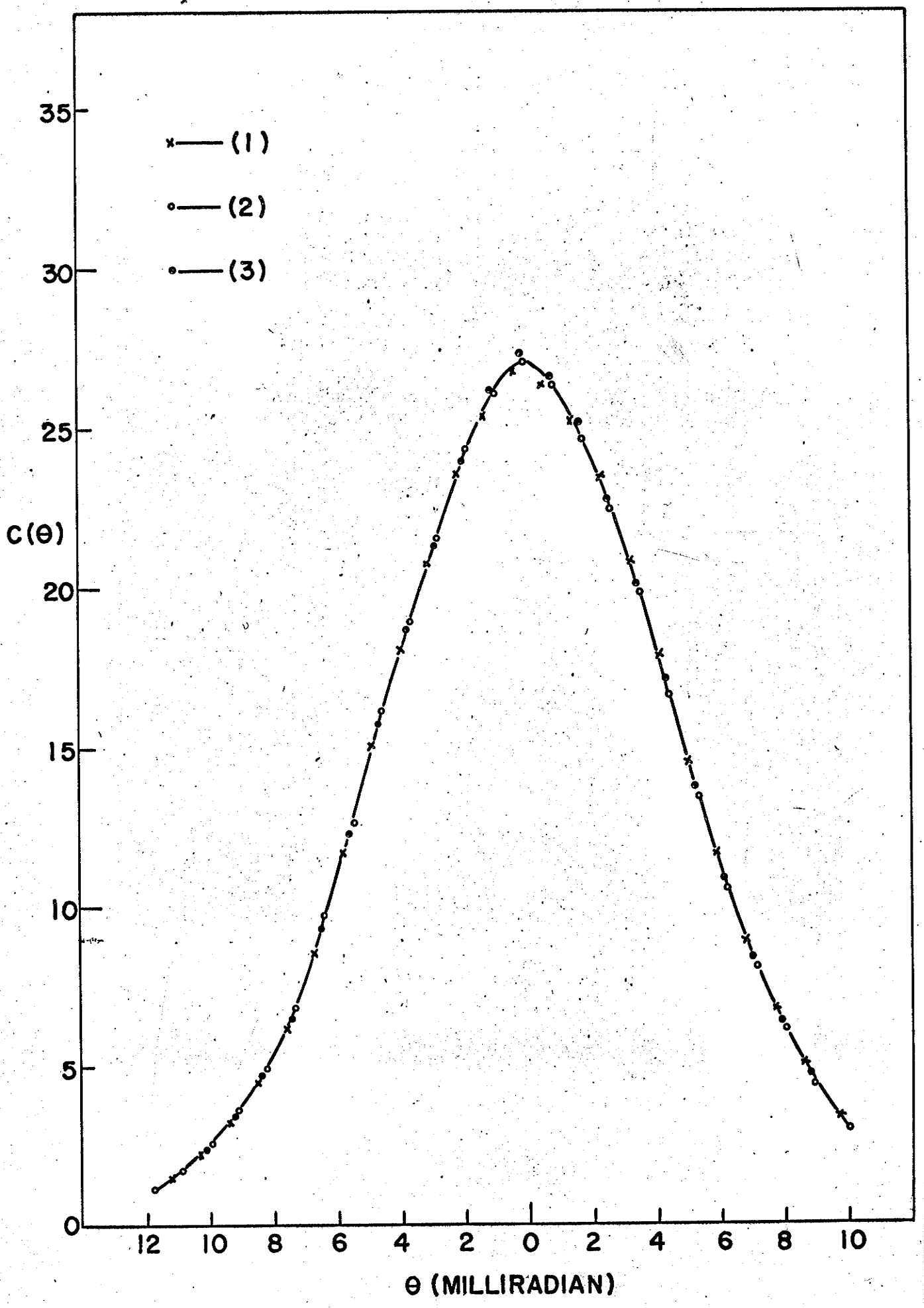
35
30
25
20
15
10
5
0
C(θ)
(1)
(2)
(3)
12
10
8
6
4
2
0
2
4
6
8
10
θ (MILLIRADIAN)

FIGURE 13

MOMENTUM DISTRIBUTIONS $N(p)$ vs θ, and
MOMENTUM SPACE DENSITY $\rho(p)$ vs θ
FOR $NaNO_3$ SOLUTION IN WATER (1 MOLE/LITER)

(1) Oxygen-saturated $NaNO_3$ Solution
(2) Air-saturated " "
(3) Degassed " "

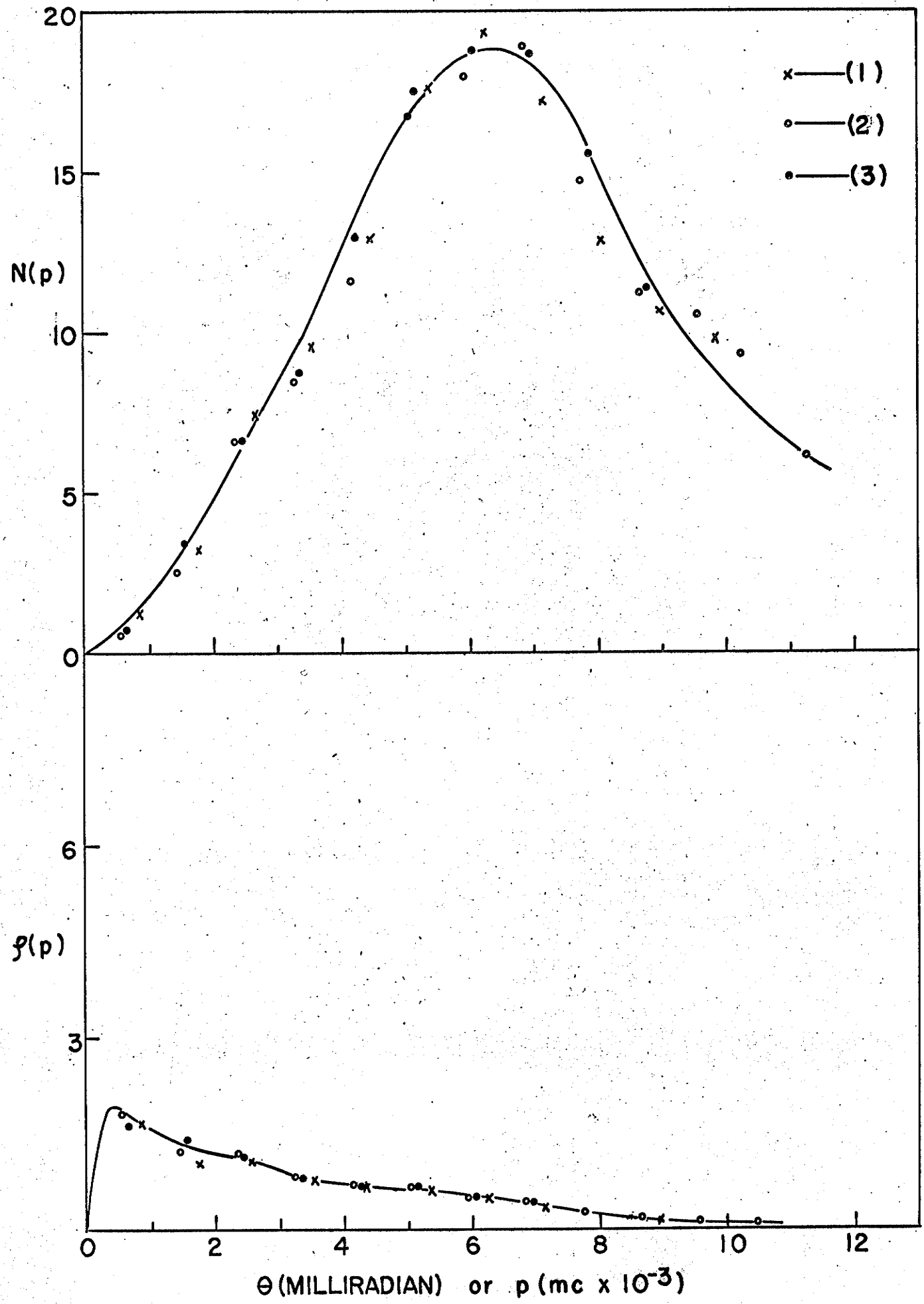
20
15
10
5
0
N(p)
×——(1)
○——(2)
•——(3)
6
3
p(p)
0
2
4
6
8
10
12
θ (MILLIRADIAN) or p (mc x 10⁻³)

TABLE 1

Sample	I_L (%)	$I_2/3$ (%)	τ_2 (nsec)
Hexane(O_2-saturated)	15±3	----	1.0±0.2
Hexane(Air-saturated)	14±2	11.7±0.7	2.4±0.1
Hexane(Degassed)	14±3	11.1±0.7	4.0±0.1
Florohexane(O_2-saturated)	8±2	----	1.0±0.2
Florohexane(Air-saturated)	8±2	7.3±0.7	2.4±0.1
Florohexane(Degassed)	8±2	7.0±0.7	3.0±0.1
Chlorohexane(O_2-saturated)	3±2	----	1.1±0.2
Chlorohexane(Air-saturated)	3±2	4.0±0.7	2.4±0.1
Chlorohexane(Degassed)	3±2	4.7±0.7	2.9±0.1
Water	7±2	7.0±1	1.8±0.7

CHAPTER 4

PRELIMINARY INVESTIGATIONS ON POLARIZED POSITRON ANNIHILATION IN MAGNETIZED SUBSTANCES

General

Recently Mijnarends and Hambro (1964) reported some measurements on positron annihilation in magnetized single crystals of iron. It was stated that the conduction electrons in iron were polarized antiparallel to the 3d electrons. Berko and Zuckerman (1964) also announced new, independent measurements in iron and nickel in which they obtained a reasonable agreement with Mijnarends' and Hambro's results. They interpreted the results in a different manner, but still obtained evidence for the existence of such an antiparallel conduction band polarization.

Following Berko and Zuckerman, we have performed the same type of measurements with a magnetized Alnico. The results will be described in the last part of this chapter.

To further study this problem, it was suggested that a special sample having ferromagnetic properties

but without conduction electrons be investigated and compared with the ordinary ferromagnets. Therefore, ferromagnetic crystals of $(La_{.70}Pb_{.30})MnO_3$, were obtained from the solid state Materials Labaratory, Airtron Company, New Jersey, (through the good offices of Dr. A. H. Morrish), and used as a sample for investigation.

X-ray Lining up and Determination of the Structure of $(La_{.70}Pb_{.30})MnO_3$ Crystals:

If the crystals under investigation in the angular correlation measurements were not aligned, each crystal would give different results. The faces of the crystals were examined under the X-ray spectrometer. It was found that the X-ray pictures of all faces of the crystal were reasonably identical. For the further determination of the structure, an X-ray powder picture was taken. Comparing this picture with the other pictures of cubic crystals, it was determined that this crystal had a nearly cubic structure with a slight distortion. But such a distortion was so small that it would not affect the results of the angular correlation measurements.

Our result of the X-ray determination of the

FIGURE 14

UNIT CELL OF PEROVSKITE ABO_3

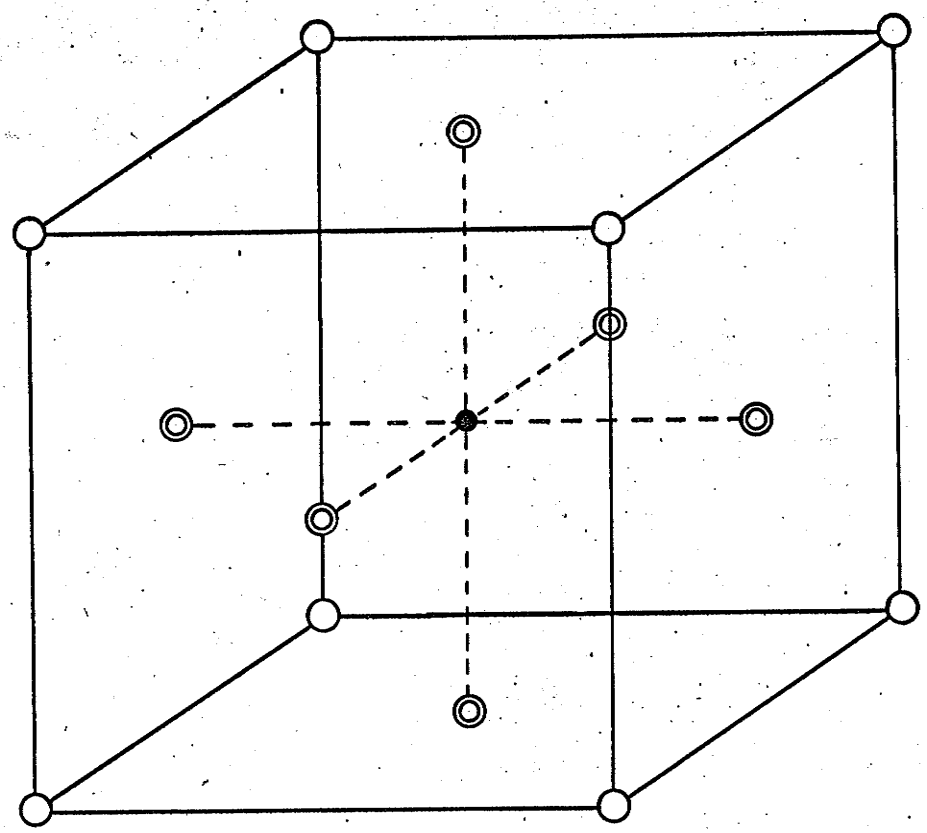

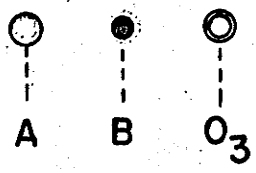
A
B
O_3

structure of $(La_{.70}Pb_{.30})MnO_3$ crystals was in agreement with the previous investigations by Jonker and van Santen (1950; 1953; 1956; Jonker 1954) in which they found that the mixed ferromagnetic compounds of manganese, such as

$La^{3+}Mn^{3+}O_3^{2-} - Ca^{2+}Mn^{4+}O_3^{2-}$, $La^{3+}Mn^{3+}O_3^{2-} - Pb^{2+}Mn^{4+}O_3^{2-}$,

$La^{3+}Mn^{3+}O_3^{2-} - Sr^{2+}Mn^{4+}O_3^{2-}$ etc, had mostly the perovskite structure. Following Jonker and van Santen, the perovskite structure of manganites, eg. $LaMnO_3$ and $PbMnO_3$, is shown in Fig. 14, in which the unit cell of a perovskite ABO_3 is given. Here "A" denotes a large ion like La^{3+} and Pb^{2+}; "B" denotes a small ion like Mn^{3+} and Mn^{4+}. The A ions are situated at the cornors of the unit cell; the B ion occupying the center of the cube while oxygen ions are placed at the centers of the faces.

Mounting of crystals

Since we have determined by X-ray spectrometry that the faces of the crystals, $(La_{.70}Pb_{.30})MnO_3$, are all identical, we can simply choose any smooth face of the crystals as the sample for investigation. Since the crystals are so small that we could not use only one, we had to put several crystals together as close as possible

by using a special wax. The smooth faces of the crystals under investigation were placed in the same plane. The bottom of the sample was mounted onto the face of a permanent magnet which provided enough magnetic field (300 G) to saturate the sample.

Results and Discussion

For each sample under investigation, two counting rates $C_{\uparrow\uparrow}(\theta)$ and $C_{\uparrow\downarrow}(\theta)$ were obtained with the magnetic field being set parallel ($\uparrow\uparrow$) and antiparallel ($\uparrow\downarrow$) respectively to the incident positron momentum. Following Berko and Zuckerman (1964), we assume that the total 2γ annihilation probability hardly changes when the field is reversed, i.e, $\int C_{\uparrow\uparrow}(\theta)d\theta = \int C_{\uparrow\downarrow}(\theta)d\theta$ within these limits. Therefore, the $C_{\uparrow\uparrow}(\theta)$ and $C_{\uparrow\downarrow}(\theta)$ curves have been normalized to the same area. (We find experimentally that the areas under the $C_{\uparrow\uparrow}(\theta)$ and $C_{\uparrow\downarrow}(\theta)$ curves are indeed equal to within 0.3% in the case of Alnico. (But in the case of $(La_{.70}Pb_{.30})MnO_3$, the difference between areas under the $C_{\uparrow\uparrow}(\theta)$ and $C_{\uparrow\downarrow}(\theta)$ curves is up to 5%; the number of counts in the low momentum area in the $C_{\uparrow\uparrow}(\theta)$ curve are obtained more than in the $C_{\uparrow\downarrow}(\theta)$ curve, but in the higher momentum area the counting rates in both $C_{\uparrow\uparrow}(\theta)$ and $C_{\uparrow\downarrow}(\theta)$ are almost the same.) The background distribution has been

subtracted in all angular correlation curves. The angular resolution was 1.0 mrad; the results have not been corrected for this. The statistical errors for the experimental points were smaller than 1%.

Figure 15 shows $C_{\uparrow\uparrow}(\theta)$ and $C_{\uparrow\downarrow}(\theta)$ (left hand scale) and the polarization $P(\theta)=\left[C_{\uparrow\uparrow}(\theta)-C_{\uparrow\downarrow}(\theta)\right]/\left[C_{\uparrow\uparrow}(\theta)+C_{\uparrow\downarrow}(\theta)\right]$ (right hand scale) for magnetized Alnico. It is seen that $P(\theta)$ changes sign for $\theta<\theta_f$, where θ_f is the angle corresponding to the free Fermi momentum based on one electron per atom in the conduction band. This is in agreement with the results for Fe crystals (Mijnarends and Hambro 1964; Berko and Zuckerman 1964). In Fig. 16 an inverted parabola, corresponding to free conduction electrons, is fitted to the $C_{\uparrow\downarrow}(\theta)$ curve for Alnico. (The rest of the curve is assumed to be due to 3d electrons alone. This of course neglects the small but finite contributions to the high momentum part of $C_{\uparrow\downarrow}(\theta)$ from the 3p and 3s electrons as well as from a more realistic conduction band.)

Following Berko's and Zuckerman's model,

$$P(\theta) = \frac{C_{\uparrow\uparrow}(\theta) - C_{\uparrow\downarrow}(\theta)}{C_{\uparrow\uparrow}(\theta) + C_{\uparrow\downarrow}(\theta)} \qquad (1)$$

and

$$C_{\uparrow\uparrow,\uparrow\downarrow} = \frac{(1+P_p)\sum_l (1\mp P_l) n_l(\theta)}{2\sum_l (1\mp P_l) W_l} + \frac{(1-P_p)\sum_l (1\pm P_l) n_l(\theta)}{2\sum_l (1\pm P_l) W_l} \qquad (2)$$

where P_p and P_1 are the positron and 1^{th} electron polarizations; $n_1(\theta)$ is the number of positron - 1^{th} electron annihilating pairs whose z-component of momentum is p_z, and $n_1(p_z=mc\theta)= \int \rho_1(\underline{p})dp_x dp_y$ in which $\rho_1(\underline{p})$ is the momentum space density and proportional to $\left|\int \psi_1(\underline{r})\, \psi_+(\underline{r}) e^{-i\underline{p}\cdot\underline{r}} d\underline{r}\right|^2$ where ψ_+ and ψ_1 are the wave functions of positron and 1^{th} electron respectively; and $W_1=\int n_1(\underline{p})dp_z$.

If one simply assumes seven 3d electrons and one conduction electron per atom (P_d=-0.3, P_s=+0.3 at room temperature) and assumes an estimated P_p=0.7, from equations (1) and (2) one indeed obtains a reversal in sign of $P(\theta)$ for $\theta<\theta_f$. Therefore, the shape of $P(\theta)$ for Alnico (as well as for Fe) seems to indicate that the conduction electrons are polarized antiparallel to the 3d electrons.

Figure 17 shows $C_{\uparrow\uparrow}(\theta)$ and $C_{\uparrow\downarrow}(\theta)$ (left hand scale) and $P(\theta)$ (right hand scale) for $(La_{.70}Pb_{.30})MnO_3$. The shapes of the $C_{\uparrow\uparrow}(\theta)$ and $C_{\uparrow\downarrow}(\theta)$ curves are slightly different. The maximum split of these two curves is about 2% of the peak counting rate, while the experimental error limit is less than 1%.

In Alnico as well as in Fe, there is an inverted parabolic portion of the curve which breaks off at θ_f.

In the $(La_{.70}Pb_{.30})MnO_3$, there is no such shape for the angular correlation. This is in agreement with the idea that there are few conduction electrons in this substance. The resistivity of $(La_{.70}Pb_{.30})MnO_3$ is larger than 10^{-2} ohm-cm (Jonker 1954; Jonker and van Santen 1956), while the resistivity of Fe and Alnico are about 10^{-5} ohm-cm (from Handbook of Chemistry and Physics). Whereas there is a change of polarization in the normal ferromagnetic metals if there is a change of polarization in $(La_{.70}Pb_{.30})MnO_3$ it is the opposite sense to Alnico and Fe,

Experiments are continuing on temperature variation of $(La_{.70}Pb_{.30})MnO_3$ and on other compounds of an ionic nature which are ferromagnetic.

FIGURE 15

$C_{\uparrow\uparrow}(\theta)$, $C_{\uparrow\downarrow}(\theta)$ vs θ (LEFT HAND SCALE)

AND $P(\theta)=\frac{C_{\uparrow\uparrow}(\theta)-C_{\uparrow\downarrow}(\theta)}{C_{\uparrow\uparrow}(\theta)+C_{\uparrow\downarrow}(\theta)}$ vs θ (RIGHT HAND SCALE)

FOR ALNICO

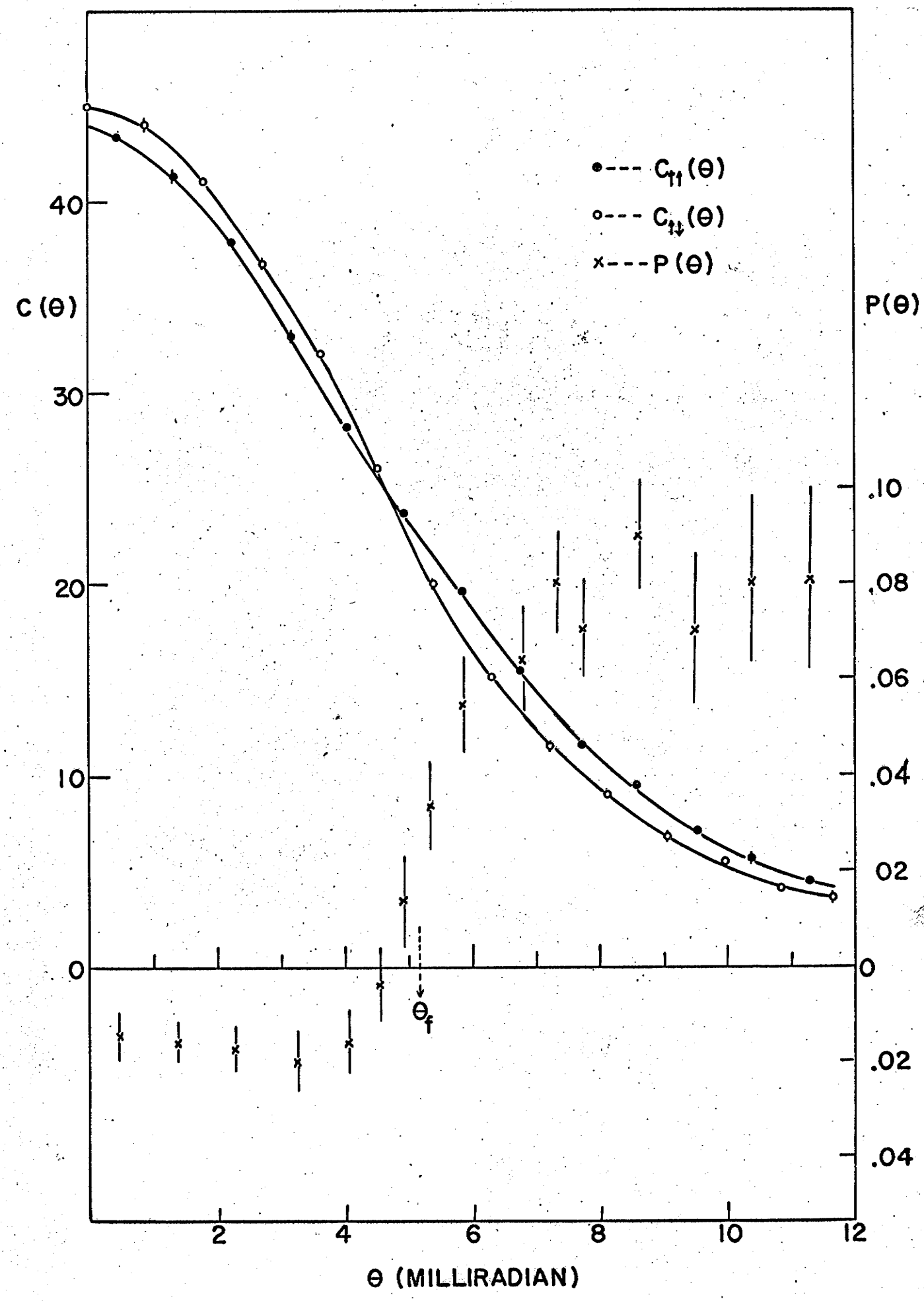
●--- $C_{\uparrow\uparrow}(\theta)$
○--- $C_{\uparrow\downarrow}(\theta)$
×---P(θ)
C(θ)
P(θ)
40
30
20
10
0
.10
.08
.06
.04
02
0
.02
.04
θ_f
2
4
6
8
10
12
θ (MILLIRADIAN)

FIGURE 16

DECOMPOSITION OF $C_{\uparrow\downarrow}(\theta)$ FOR ALNICO (1) INTO A CONDUCTION BAND (2) AND A 3d BAND (3) CONTRIBUTION

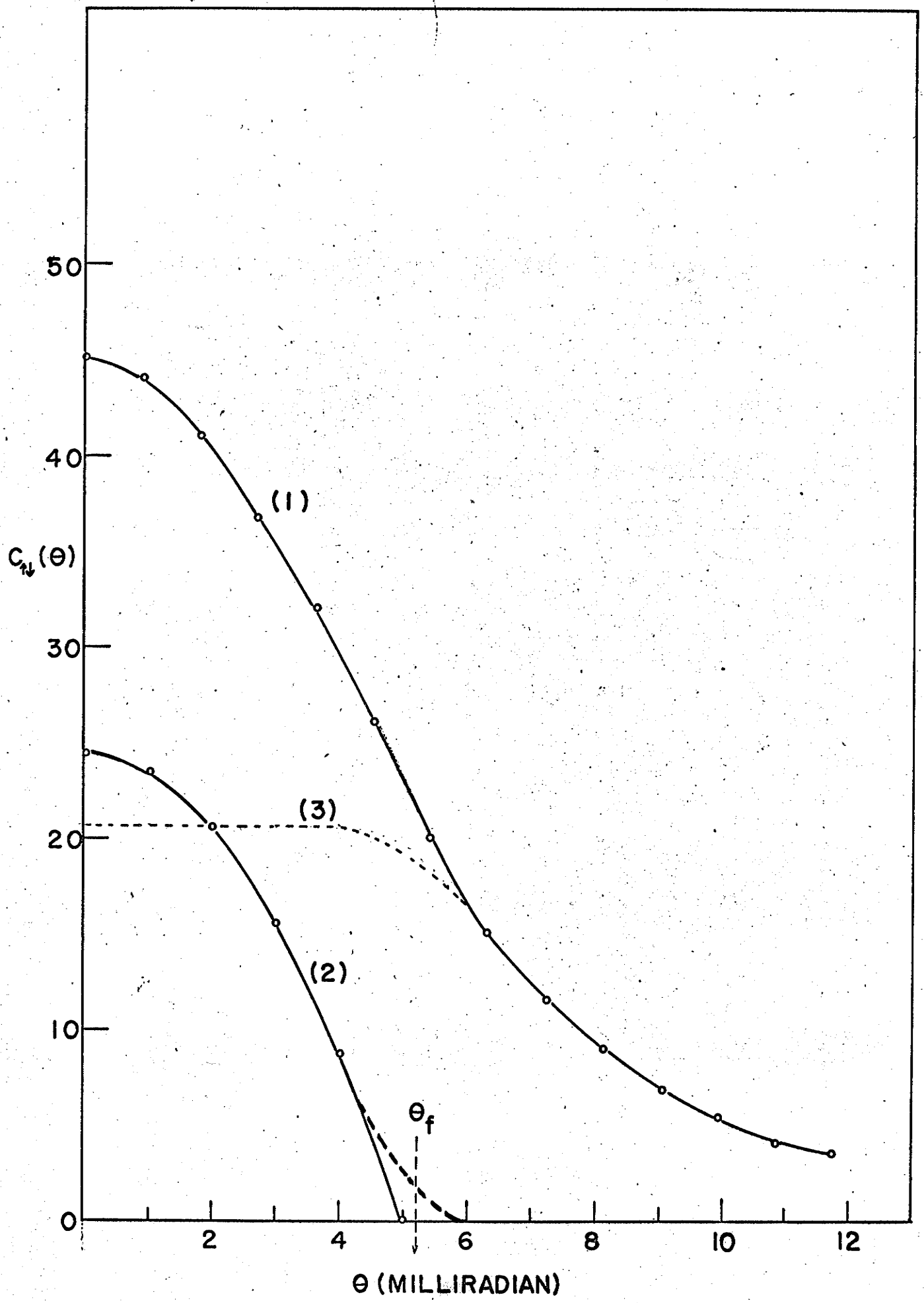
50
40
30
20
10
0
$C_{\uparrow\downarrow}(\theta)$
(1)
(2)
(3)
θ_f
2
4
6
8
10
12
θ (MILLIRADIAN)

FIGURE 17

$C_{\uparrow\uparrow}(\theta)$, $C_{\uparrow\downarrow}(\theta)$ vs θ (LEFT HAND SCALE)

AND $P(\theta)=\frac{C_{\uparrow\uparrow}(\theta)-C_{\uparrow\downarrow}(\theta)}{C_{\uparrow\uparrow}(\theta)+C_{\uparrow\downarrow}(\theta)}$ vs θ (RIGHT HAND SCALE)

FOR $(La_{.70}Pb_{.30})MnO_3$

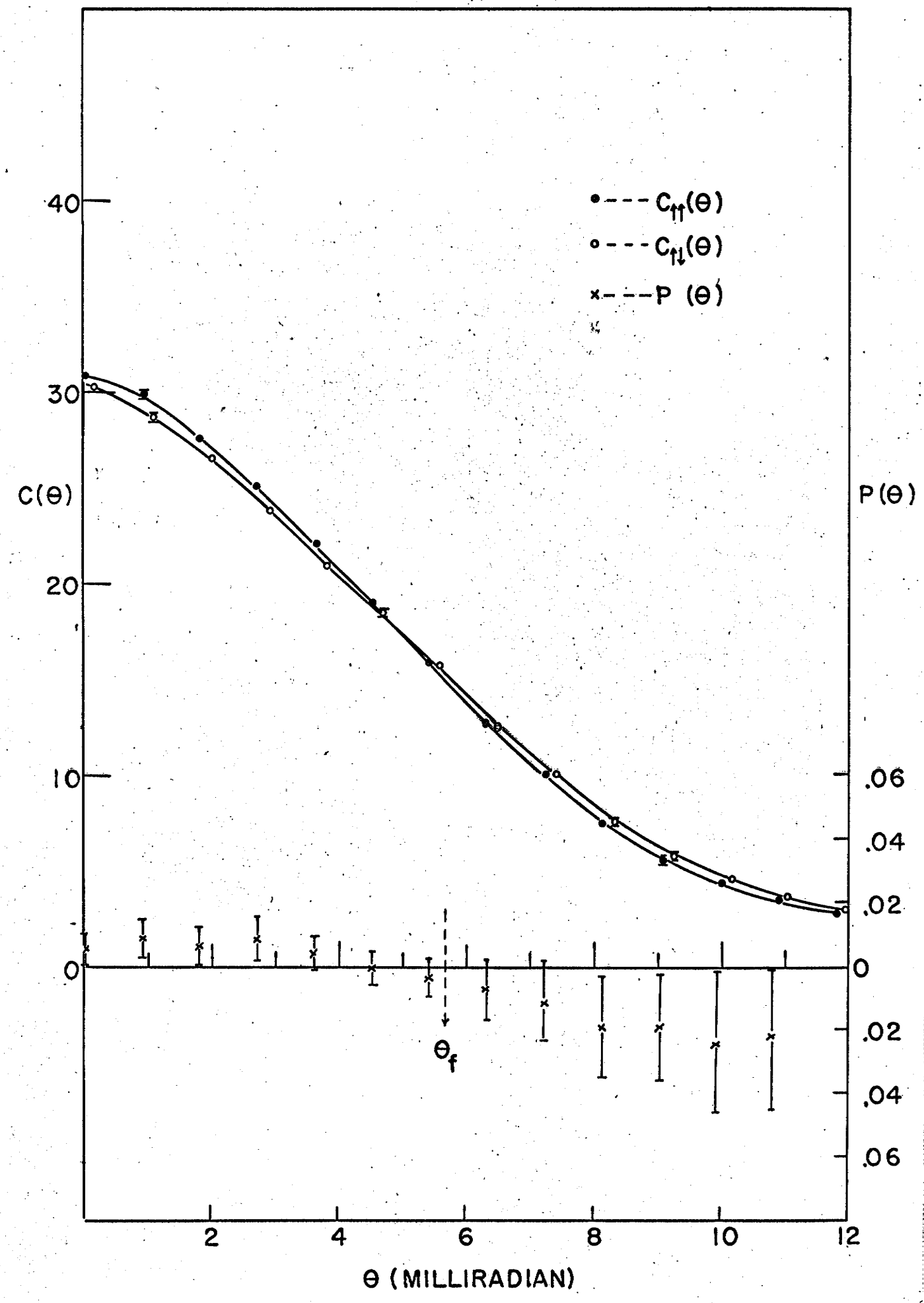
$C_{\uparrow\uparrow}(\theta)$
$C_{\uparrow\downarrow}(\theta)$
$P(\theta)$
40
30
20
10
0
C(θ)
P(θ)
.06
.04
.02
0
.02
.04
.06
θ_f
2
4
6
8
10
12
θ (MILLIRADIAN)

REFERENCES

ARGYLE, P.E. and WARREN, J.B. 1951. Can. J. Phys. 29, 32.

BERINGER, R. and MONTGOMERY, C.G. 1942. Phys. Rev. 61, 222.

BERKO, S. and ZUCHELL, A.J. 1956. Phys. Rev. 102, 724.

BERKO, S. and ZUCKERMAN, J. 1964. Phys. Rev. Letters Vol. 13 No. 11, 339.

COOPER, A.M. 1965. Master Thesis, University of Manitoba.

DE BENEDETTI, S., COWAN, C.E., KONNEKER,W.R., and PRIMAKOFF, H. 1950. Phys. Rev. 77, 205.

DE ZAFRA, R.L. 1958. Univ. of Maryland, Phys, Dept. Technical Report No. 108.

DONAGHY,J.J. and STEWART, A.T. 1964. Bull. Am. Phys. Soc. 9, 238.

DRESDEN, M. 1954. Phys. Rev. 93, 1413.

ERDMAN, K.L. 1955. Proc. Phys. Soc. 68, 304.

FERRELL, R.A. 1956. Univ. of Maryland, Phys. Dept. Technical Report No. 98.

GREEN, R.E. and STEWART, A.T. 1955. Phys. Rev. 98, 486.

HANNA, S.S. and PRESTON, R.S. 1958. Phys. Rev. 109, 716.

JONKER, G.H. and VAN SANTEN, J.H. 1950 Physica 16, 337.

JONKER, G.H. and VAN SANTEN, J.H. 1953. Physica19, 120.

JONKER, G.H. 1954. Physica 20, 1118.

JONKER, G.H. 1956. Physica 22, 707.

KERR,D.P. 1964. Ph.D. Thesis, University of Manitoba.

KERR, D.P.,,COOPER, A.M. and HOGG, B.G. 1965. Can. J. Phys. 43, 963.

LANG, G., DE BENEDETTI, S., and SMOLUCHOWSKI, R. 1955. Phys. Rev. 99, 596(L).

LEE. J. and CELITANS, G.J. 1965. J. Chem. Phys. (in press).

MAIER-LEIBNITZ, H. 1951. Z. Naturforsch 6a, 663.

MIJNARENDS, P.E. and HAMBRO, L. 1964. Phys. Letters 10, No. 3, 272.

NAQVI, S.I.H. 1961. Ph.D. Thesis, University of Manitoba.

PAGE, L.A. and HEINGERG, M. 1956. Phys. Rev. 102, 1545.

PAGE, L.A., HEINBERG, M., WALLACE, J., and TROUT, T. 1955. Phys. Rev. 98, 206(L).

PAUL, D.A.L. 1958. Can. J. Phys. 36, 640.

STEWART, A.T. 1955. Phys. Rev. 99, 596(L).

STEWART, A.T. 1957. Can. J. Phys. 35, 168.

STEWART, A.T. and GREEN, R.E. 1955. Phys. Rev. 98, 232(A).

STEWART, A.T., and POPE, N.K. 1960. Phys. Rev. 120, 2033.

TRUMPY, G. 1960. Phys. Rev. 118, 668.

WALLACE, P.R. 1960. "Solid State Physics" (Academic Press, New York) Vol. 10.

WALLACE, P.R. 1955. Phys. Rev. 100, 738.

WARREN, J.B. and GRIFFITHS, G.M. 1951. Can. J. Phys. 29, 325.